

uncertainties. We have no explanation, but it is widely recognized that the differences between experimental and calculated amplitudes are subject to greater fluctuations than, say, are structural differences obtained by different structural methods. In any case, these amplitude differences do not affect our conclusions about the structure.

**Acknowledgment.** This work was supported by the National Science Foundation under Grant CH84-11165. We thank Pro-

fessor K. Wiberg and Dr. W. Dailey for the sample of [1.1.1]-propellane.

Registry No. [1.1.1]Propellane, 35634-10-7.

**Supplementary Material Available:** From each plate: tables of total intensities, final backgrounds, and molecular intensities (9 pages). Ordering information is given on any current masthead page.

## Theoretical Study of the Stability of Molecular $P_2$ , $P_4$ ( $T_d$ ), and $P_8$ ( $O_h$ )

Reinhart Ahlrichs,\* Stefan Brode, and Claus Ehrhardt

Contribution from the Institut für Physikalische Chemie und Elektrochemie, Lehrstuhl für Theoretische Chemie, Universität Karlsruhe, 7500 Karlsruhe, West Germany.

Received February 21, 1985

**Abstract:** Results of ab initio calculations are reported for  $P_2$ ,  $P_4$ , and  $P_8$  on the SCF level and with inclusion of valence correlation effects, except for  $P_8$ . Extended polarization basis sets are employed, up to (3d2f1g) for  $P_2$ , (2d1f) for  $P_4$ , and (1d) for  $P_8$ .  $R_e$  values obtained on the highest level of theory are in excellent agreement with experiment (in parentheses):  $R_e(P_2) = 189.6$  pm (189.4),  $R_e(P_4) = 221$  pm ( $221 \pm 2$ ). Computed reaction energies still suffer from basis saturation problems,  $D_e(P_2) = 437$  kJ/mol (490),  $\Delta E(P_4 \rightarrow 2P_2) = 201$  kJ/mol (232).  $P_8$  is computed to be less stable than  $2P_4$  by 158 kJ/mol. The remarkable stability of  $P_4$  is attributed to (i) a relatively small strain energy arising from  $60^\circ$  bond angles and (ii) stabilizing multicenter bonding closely connected to enhanced 3d contributions (as compared to  $P_8$ ), which are typical for three-membered rings.  $P_8$  is destabilized by the repulsion between parallel PP bonds.

### I. Introduction

The remarkable stability of the tetrahedral  $P_4$  molecule constitutes one of the so far not well understood peculiarities of the chemistry of phosphorus and other group V elements such as arsenic.<sup>1</sup> Despite the strain expected for  $60^\circ$  bond angles, one finds a P-P bond energy of  $\approx 200$  kJ/mol in  $P_4$ , which may be considered as typical for P-P bonds.<sup>1</sup> Virtually no strain should be present in cubic  $P_8$ , but this molecule has never been observed.

Theoretical investigations have so far not been too successful to elucidate the just mentioned problems. Results of electronic structure calculations usually underestimate the stability of  $P_4$  with respect to  $2P_2$  to a considerable extent.<sup>2,3</sup> Trinquier et al.<sup>2</sup> find  $P_4$  to be 125 kJ/mol more stable than  $2P_2$  (on the DZP SCF level), as compared to the experimental value of 228 kJ/mol.<sup>4</sup> The same authors obtained  $P_8$  to be 42 kJ/mol more stable than  $2P_4$ , but it was argued quite convincingly that this result reflects merely basis set problems. The comparison of  $P_4$  and  $P_8$  could be done on the DZ SCF level only, and d functions should stabilize  $2P_4$  more than  $P_8$ .<sup>2</sup>

The availability of improved computer hardware, especially supercomputers, and of efficient program packages<sup>5</sup> now opens the way for more accurate treatments of the relative stability of  $P_2$ ,  $P_4$ , and  $P_8$  which will be reported in this work.

### II. Details of Computation

The computations were performed with the Karlsruhe version<sup>5</sup> of the Columbus system of programs,<sup>6-8</sup> which has been especially

adapted for the CYBER 205. Effects of valence electron correlation were included for the smaller systems  $P$ ,  $P_2$ , and  $P_4$  ( $P_8$  could only be treated on the SCF level) by means of the recently developed coupled pair functional method (CPF).<sup>9</sup> The CPF procedure is based on the variation of an energy functional derived from the CI(SD) energy expression by the introduction of partial normalization denominators in order to achieve size extensivity for the energy. The CPF method is related to CEPA-1<sup>10,11</sup> and has already proved useful in various applications.<sup>9,12,13</sup>

The following CGTO basis sets were employed:

$$(s,p): (11,7)/[6,4]^{14}$$

polarization sets:

(1d)

$$\eta(d) = 0.4$$

(2d1f)

$$(d) = 0.23, 0.7; \eta(f) = 0.5$$

(3d2f1g)

$$(d) = 0.167, 0.468, 1.307$$

$$\eta(f) = 0.252, 0.919$$

$$\eta(g) = 0.585$$

The (1d) orbital exponent  $\eta$  is optimal for  $P_2$  on the CPF level

(1) Kutzelnigg, W. *Angew. Chem.* **1984**, *96*, 262.  
 (2) Trinquier, G.; Malrieu, J.-P.; Daudey, J.-P. *Chem. Phys. Lett.* **1981**, *80*, 552.  
 (3) Wedig, U.; Stoll, H.; Preuss, H. *Chem. Phys.* **1981**, *61*, 127.  
 (4) Stull, D. R.; Prophet, H.; et al. "JANAF Thermochemical Tables"; Dow Chemical Corp.: Springfield, VA, 1971.  
 (5) Ahlrichs, R.; Böhm, H. J.; Ehrhardt, C.; Scharf, P.; Schiffer, H.; Lischka, H.; Schindler, M. *J. Comput. Chem.* **1985**, *6*, 200.  
 (6) Dupuis, M.; Rys, J.; King, H. F. *J. Chem. Phys.* **1976**, *65*, 111. Rys, J.; Dupuis, M.; King, H. F. *J. Comput. Chem.* **1983**, *4*, 154.

(7) Pitzer, R. M. *J. Chem. Phys.* **1973**, *58*, 3111.  
 (8) Lischka, H.; Shepard, R.; Brown, F. B.; Shavitt, I. *Int. J. Quantum Chem. Quantum Chem. Symp.* **1981**, *15*, 91.  
 (9) Ahlrichs, R.; Scharf, P.; Ehrhardt, C. *J. Chem. Phys.* **1985**, *82*, 890.  
 (10) Meyer, W. *J. Chem. Phys.* **1973**, *58*, 1017.  
 (11) Ahlrichs, R. In "Methods in Computational Molecular Physics"; Diercksen, G. H. F., Wilson, S., Eds.; Reidel: Dordrecht, 1983.  
 (12) Scharf, P.; Brode, S.; Ahlrichs, R. *Chem. Phys. Lett.* **1985**, *113*, 447.  
 (13) Ahlrichs, R.; Scharf, P.; Jankowski, K. *Chem. Phys.* **1985**, *98*, 381.  
 (14) Huzinaga, S. "Approximate Atomic Functions"; Technical Report, University of Alberta, Canada, 1971; Vol. II.

Table I. Computed Total Energies and Equilibrium Distances for  $P$ ,  $P_2$  ( $D_{\infty h}$ ),  $P_4$  ( $T_d$ ), and  $P_8$  ( $O_h$ ) on Various Levels of Approximation<sup>a</sup>

system	state	basis <sup>b</sup>	SCF		CPF	
			$R_e$	$-E$	$R_e$	$-E$
P	$^4S_u$	2d1f		340.676 81		340.779 07
P	$^4S_u$	3d2f1g		340.676 81		340.782 08
$P_2$	$^1\Sigma_g^+$	1d	3.521	681.402 62	3.636	681.657 24
$P_2$	$^1\Sigma_g^+$	2d1f	3.507	681.413 45	3.600 <sup>c</sup>	681.714 04
$P_2$	$^1\Sigma_g^+$	3d2f1g			3.583	681.730 51
$P_4$	$^1A_1$	1d	4.160	1 362.862 88	4.239	1 363.366 09
$P_4$	$^1A_1$	2d1f	4.120	1 362.896 20	4.170 <sup>d</sup>	1 363.504 71
$P_8$	$^1A_g$	1d	4.330	2 725.665 78		

<sup>a</sup>All quantities in au. <sup>b</sup>Polarization functions employed in addition to the (11,7)/[6,4] sp basis as explained in the text. <sup>c</sup>Experimental result,  $R_e = 1.894 \text{ \AA} = 3.579a_0$ .<sup>17</sup> <sup>d</sup>Experimental result,  $R_e = 221 \pm 2 \text{ pm} = 4.18a_0 \pm 0.04 a_0$ .<sup>19</sup>

Table II. Computed Reaction Energies, in kJ/mol<sup>a</sup>

reaction	method <sup>b</sup>	$\Delta E$
$P_2 \rightarrow 2P$	CPF (2d1f)	409.4
	CPF (3d2f1g)	436.8 <sup>c</sup>
$P_4 \rightarrow 2P_2$	SCF (1d)	151.4
	SCF (2d1f)	182.0
	CPF (1d)	135.5
	CPF (2d1f)	201.2 <sup>d</sup>
$P_8 \rightarrow 2P_4$	SCF (1d)	-157.5

<sup>a</sup>As obtained from the results listed in Table I. <sup>b</sup>Method of computation and basis set used, see Table I and text. <sup>c</sup>Experimental result  $D_0 = 5.03 \text{ eV} = 485.6 \text{ kJ/mol}$ ,  $D_e = 490 \text{ kJ/mol}$ .<sup>17</sup> <sup>d</sup>Experimental  $\Delta H$  at 298.15 K:  $54.59 \text{ kcal/mol} = 228 \text{ kJ/mol}$ ,  $\Delta E = 232 \text{ kJ/mol}$ .<sup>4</sup>

and for  $P_4$  on the SCF and CPF levels. (The optimized  $\eta(d)$  for  $P_2$  SCF is slightly smaller:  $\eta \approx 0.38$ .) The orbital exponents of the larger polarization sets were obtained from the (1d) by means of a proven scaling procedure.<sup>15,16</sup> Only valence orbitals were correlated in the CPF calculations, and one high-lying virtual MO per P atom was kept frozen.

### III. Energies and Equilibrium Distances

The computed electronic energies and equilibrium distances are collected in Table I and the corresponding reaction energies in Table II.

The present results for  $P_2$  mainly demonstrate the basis saturation problems encountered in CI-type treatments and show a similar state of affairs as found for first row diatomics.<sup>9,13</sup> On the (2d1f) CPF level  $R_e$  is still predicted too large by  $0.02a_0$ , and  $D_e$  too small, by  $81 \text{ kJ/mol} = 0.8 \text{ eV}$ .<sup>17</sup> The large (3d2f1g) polarization basis virtually reproduces the experimental  $R_e$ , up to  $0.004a_0$ , but yields  $D_e$  still  $53 \text{ kJ/mol}$  too small. Although further basis set extension will certainly increase the computed  $D_e$ , the CPF method appears to underestimate  $D_e$  even in the complete basis set limit.<sup>9,13</sup> The most elaborate previous calculation for  $P_2$  has been published by McLean et al.,<sup>18</sup> who performed CI(SD) calculations employing an (8,6,3,2) STO basis. Their best results were obtained if cluster corrections were included by Davidson-type procedures which yield  $D_e = 1.892$  to  $1.897 \text{ eV}$ , depending on the actual procedure used. These results,  $D_e \approx 408 \pm 7 \text{ kJ/mol}$ , are close to the present (2d1f) CPF value,  $D_e = 409 \text{ kJ/mol}$ .

It should be kept in mind that  $D_e$  is difficult to compute for diatomics, since one has to compare the energy of  $P_2$  ( $^1\Sigma_g^+$ ) with that of  $2P$  ( $^4S_u$ ). The atomic correlation energy is relatively small, and a large fraction of the correlation energy of  $P_2$  is of extra-molecular type, i.e., no appreciable cancellation of errors can be expected.

The situation is certainly much better for  $P_4$  vs.  $2P_2$  or  $P_8$  vs.  $2P_4$ , since all systems have a closed shell structure and errors due

to basis saturation effects will cancel to a much larger extent.

The computed reaction energies for  $2P_2 \rightarrow P_4$ , Table II, show somewhat unsystematic variations at first glance. On the SCF level one finds a pronounced influence of f functions:  $\Delta E$  increases from  $151 \text{ kJ/mol}$  (1d) to  $182 \text{ kJ/mol}$  (2d1f)—the second d set is of little importance as has been checked by additional calculations. The relatively large effect of f functions indicates bond strain in  $P_4$ : contributions of f (and d) functions to MOs help to increase the overlap of AOs in the case of small bond angles.

Comparing the computed SCF and CPF reaction energies for  $2P_2 \rightarrow P_4$  one finds a decrease from  $151$  to  $136 \text{ kJ/mol}$  for the (1d) set but an increase from  $182$  to  $201 \text{ kJ/mol}$  for the (2d1f) set. This may be rationalized in the following way.  $P_2$  has high-lying occupied  $\pi$  and low-lying empty  $\pi^*$  MOs, and near degeneracy effects are of great importance. The latter are already rather well described on the (1d) level. Dynamic correlation is of more importance for  $P_4$ , which requires a large polarization set for a proper description. It is thus expected that the result from the most elaborate calculation, CPF (2d1f)

$$\Delta E(P_4 \rightarrow 2P_2) = 201.2 \text{ kJ/mol} \quad (1)$$

should increase on further basis set extension. This would reduce the remaining discrepancy to the experimental result

$$\Delta E = 232 \pm 2 \text{ kJ/mol} \quad (2)$$

which is obtained from the  $\Delta H_f^\circ$  of  $P_2$  and  $P_4$  with the aid of the known  $\omega_e$ .<sup>4</sup>

The (2d1f) CPF result for  $R_e$

$$R_e(P_4) = 4.17a_0 = 221 \text{ pm} \quad (3)$$

is in perfect agreement with the only available experimental value of  $221 \pm 2 \text{ pm}$ .<sup>19</sup> Since further basis set extension is expected to decrease the computed  $R_e$ , as has been discussed above for  $P_2$ , the present results suggest

$$R_e(P_4) = 219.7 \pm 0.5 \text{ pm} \quad (4)$$

as the most probable value.

The present results finally show cubic  $P_8$  to be markedly less stable than  $2P_4$ , by  $158 \text{ kJ/mol}$  on the (1d) SCF level. It is hard to imagine that this energetic ordering could be reversed by employing more extended basis sets or by effects of electron correlation. It should be noted that one rather expects  $P_4$  to be more stabilized than  $P_8$  if f functions are included. The unusually large P-P distance

$$R_e(P_8) = 4.33a_0 = 229 \text{ pm} \quad (5)$$

obtained on the SCF level also indicates  $P_8$  to be rather high in energy and reactive. Some additional calculations were performed with the relatively small (11,7)/[6,4] basis set. Cubic  $P_8$  was found to be stable against distortions within  $D_{2d}$  symmetry on the SCF level. (A quadratic antiprism leads to a triplet ground state—two electrons in the e-type HOMO—which is hardly expected to be a stable and nonreactive molecular state.) Effects of electron correlation (on the CPF level for the small basis) increased the

(15) Ahlrichs, R.; Taylor, P. *Chem. Phys.* **1982**, *72*, 287.

(16) Ahlrichs, R.; Keil, F.; Lischka, H.; Kutzelnigg, W.; Staemmler, V. *J. Chem. Phys.* **1975**, *63*, 455.

(17) Huber, K. P.; Herzberg, G. "Constants of Diatomic Molecules"; van Nostrand: New York, 1979.

(18) McLean, A. D.; Liu, B.; Chandler, G. S. *J. Chem. Phys.* **1984**, *80*, 5130.

(19) Maxwell, L. R.; Hendrichs, S. B.; Mosley, V. *J. Chem. Phys.* **1935**, *3*, 699.

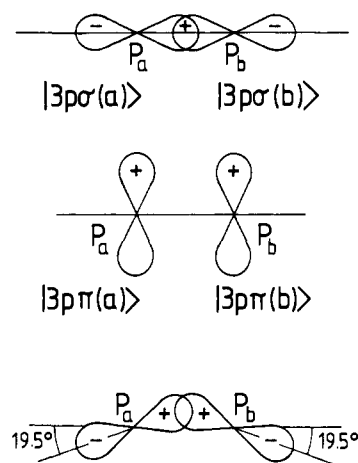


**Figure 1.** Schematic representation and phase convention of MOs describing a PP  $\sigma$  bond (a),  $\pi$  bond (b), and a banana (c) bond as described in the text.

energetic separation between  $P_8$  and  $2P_4$ . Although small basis set results should be considered with care, the additional calculations strongly indicate that the instability of  $P_8$  with respect to  $2P_4$  is not just an artefact of the SCF method.

#### IV. Electronic Structure of $P_4$ and $P_8$

The experimental as well as the present theoretical results show the presence of six normally strong PP bonds in  $P_4$ : a bond energy of  $\approx 200$  kJ/mol (one-sixth of the atomization energy) and a bond distance of 220 pm.  $P_8$  is computed to be 158 kJ/mol higher in energy than  $2P_4$ , Table II, which implies its PP bonds to be 13 kJ/mol or 6% less stable than those in  $P_4$ . This situation appears to be typical for phosphorus chemistry for which  $P_3$  (as well as  $P_5$  and  $P_6$ ) rings are quite common<sup>20</sup> whereas  $P_4$  rings are rather exceptional. This makes it worthwhile to analyze the electronic structure of  $P_4$  and  $P_8$  in more detail. For this purpose we will attempt to assess in a semiquantitative way the most likely effects coming into play: bond strain arising from  $60^\circ$  angles in  $P_4$ , repulsion between bonds (especially in  $P_8$ ), and the role of 3d participation.

Some useful facts are provided by the results of the Mulliken population analysis<sup>21</sup> which yields the following valence shell gross occupations at the  $R_e$  given in eq 3 and 5.

$$P_4: 3s^{1.85}3p^{2.95}3d^{0.20}(4f^{0.02}) \quad (6)$$

$$P_8: 3s^{1.80}3p^{3.06}3d^{0.14} \quad (7)$$

Deviations from the free atom occupations  $3s^23p^3$ , are small. Bonding in  $P_4$  and  $P_8$ —like in other normal valent P compounds—involves mainly the 3p AOs, as expected. However, hybridization is slightly more pronounced in  $P_8$ , where 3s electrons are promoted into 3p and 3d, whereas 3s and 3p electrons are promoted into 3d AOs in  $P_4$ .

In order to get more detailed informations we have performed additional SCF calculations designed to quantify—as much as possible—effects of bond strain, bond repulsions, and 3d participation, which will be discussed in subsections a–c.

**(a) The  $\sigma(3p)$  Model.**<sup>22</sup> In these calculations we have enforced  $\sigma$  bonds constructed from 3p AOs;<sup>23</sup> the corresponding bond orbitals will be denoted  $\sigma(3p)$ . The construction of  $\sigma(3p)$  is straightforward for cubic  $P_8$  where bonds are aligned along the PP axes, as shown schematically in Figure 1a. For  $P_4$  one is led

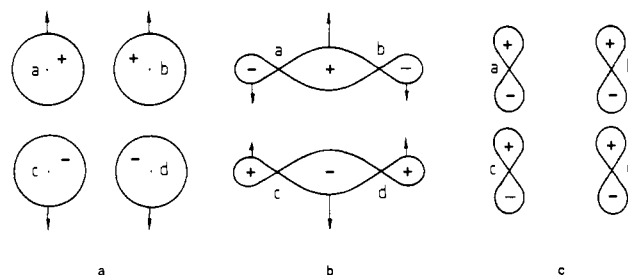


**Figure 2.** Schematic representation of the polarizing effects of a  $\sigma^*(3p)$  admixture to MOs for a  $P_4$  ring. a and b depict MOs constructed from 3s AOs and  $\sigma(3p)$  bond orbitals, which are bonding between centers a–b and c–d and antibonding between a–c and b–d. These MOs interact with  $\sigma^*(3p)$  orbitals of bonds a–c and b–d, shown in c. The polarizing effect on the MOs in parts a and b is indicated by arrows.

to bent or banana bond orbitals, denoted |BB>, which have the explicit representation, in the nomenclature of Figure 1

$$|BB\rangle = N\{[3p\sigma(a) + 3p\sigma(b) + 1/8^{1/2}\{[3p\pi(a) + 3p\pi(b)]\}] \quad (8)$$

The structure of |BB> is uniquely determined by the requirement that the six PP bonds in  $P_4$  should be equivalent.

The  $\sigma(3p)$  model suppresses hybridization: the  $\sigma(3p)$  orbitals are doubly occupied, yielding a gross occupation of 1.0 for either 3p AO and a total valence occupation  $3s^23p^3$ , as in the free atom.

The  $\sigma(3p)$  model predicts  $P_4$  to be markedly more stable than  $P_8$  at the typical PP distance of 222 pm assumed for either molecule.

$$\sigma(3p) \text{ model: } E(P_8) - 2E(P_4) = 556 \text{ kJ/mol} \quad (9)$$

The energy difference has to be attributed to effects of bond strain and bond repulsions—since the molecules are treated on the same footing in all other respects—and it shows bond repulsion effects in  $P_8$  to outweigh considerably the possible strain in  $P_4$ . An estimate of the bond strain in  $P_4$  can be obtained from the structure of |BB>, eq 8. |BB> has  $\approx 89\%$   $\sigma$  character ( $\sigma$  bond strength  $\approx 200$  kJ/mol<sup>1</sup>) and  $\approx 11\%$   $\pi$  character ( $\pi$  bond strength  $\approx 100$  kJ/mol<sup>1</sup>), which leads to a bond strength of  $\approx 190$  kJ/mol for a banana bond |BB>. This implies a bond strain of only about 10 kJ/mol per bond and

$$\text{total bond strain of } P_4 \approx 60 \text{ kJ/mol} \quad (10)$$

The surprisingly small strain energy basically results from the fact that bonding in  $P_4$  involves dominantly the 3p AOs.

An enormous bond repulsion of about 680 kJ/mol is suggested for  $P_8$  within the  $\sigma(3p)$  model according to eq 9 and 10. Adjacent parallel bonds in  $P_8$  should in fact repel each other quite strongly since they are separated by a PP bond distance only ( $\approx 222$  pm), which is much smaller than the PP van der Waals distance (360 pm). Since 12 such interactions are present in  $P_8$ , one gets a rough estimate of  $\approx 57$  kJ/mol ( $=680/12$ ) for the repulsion between adjacent parallel  $\sigma(3p)$  bonds.

**(b) The  $\sigma(3p)$  Plus  $\sigma^*(3p)$  Model.** Next we performed calculations which included the  $\sigma^*(3p)$  orbitals in addition to  $\sigma(3p)$ , i.e., all 3p AOs were included in the basis set. The  $\sigma^*(3p)$  orbitals lead only to a minor lowering of the SCF energy of  $P_4$ , by 112 kJ/mol, but to a drastic stabilization of  $P_8$ , by 742 kJ/mol.  $P_8$  is now only marginally less stable than  $P_4$

$$\sigma(3p) \text{ plus } \sigma^*(3p): E(P_8) - 2E(P_4) = 39 \text{ kJ/mol} \quad (11)$$

again at  $R = 222$  pm for both molecules.  $P_8$  is even more stable than  $P_4$  on this level if  $R$  is optimized, in agreement with the result of Trinquier et al.<sup>2</sup> The modest stabilization of  $P_4$  by  $\sigma^*(3p)$  orbitals indicates this molecule to be rather well described by the  $\sigma(3p)$  model.

The contributions of  $\sigma^*(3p)$  orbitals are obviously very effective in reducing bond repulsions in  $P_8$ . The corresponding mechanism is depicted schematically in Figure 2 for the case of a quadratic  $P_4$  ring. Since  $\sigma^*(3p)$  orbitals have a nodal surface passing through

(20) Baudler, M. *Angew. Chem.* **1982**, *94*, 520.

(21) Mulliken, R. S. *J. Chem. Phys.* **1955**, *23*, 1833.

(22) The present analysis is related to the semiempirical LCBO (linear combination of bond orbitals) method. For a recent article we refer to: Wesenberg, G.; Weinhold, F. *Int. J. Quant. Chem.* **1982**, *21*, 487.

(23) This was achieved by a generalized contraction of the 7p basis to 3 CGTOs representing the SCF 2p AO and the 3p AO in a split valence contraction. All symmetry orbitals arising from 2p AOs were kept but from the 3p AO only those corresponding to  $\sigma(3p)$  orbitals were included in the basis.

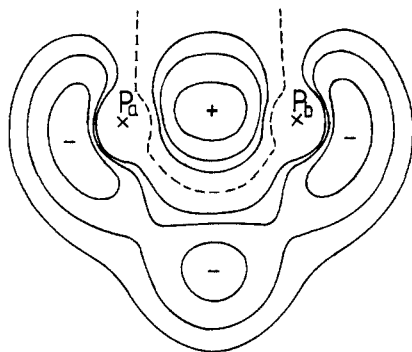


**Figure 3.** Contour lines of the highest occupied  $t_2$  MO of  $P_4$  in the plane going through the center of the tetrahedron and two corners occupied by  $P_a$  and  $P_b$ .  $P_c$  and  $P_d$  are above and below the plane in the lower part of the figure. The lines plotted correspond to 0 (dashed),  $\pm 0.04$ ,  $\pm 0.06$ ,  $\pm 0.09$  au.

the bond center, they interact only with MOs showing a corresponding node. (This holds strictly for highly symmetric molecules, e.g., cubic  $P_8$ , and in an approximate way for lower symmetries.) The effect of  $\sigma^*(3p)$  admixture is clearly to polarize density out of the nodal area and thus to relieve the destabilizing effect of the nodal surface.

The net effect of the  $\sigma^*(3p)$  admixture is in any case that the originally straight  $\sigma(3p)$  bonds assume a slightly bent shape in order to reduce repulsion effects. In this context it should be noted that the  $\sigma^*(3p)$  contributions, Figure 2c, which polarize the minus combination of  $\sigma(3p)$  orbitals, Figure 1b, are of  $\pi$  type with respect to these  $\sigma(3p)$  orbitals, which justifies to speak of a  $\sigma-\pi$  interaction. The admixture of  $\sigma^*(3p)$  orbitals to MOs originally formed from 3s AOs is responsible for the slight hybridization discussed in connection with the results of the population analysis.

**(c) Importance of 3d Participations.** The most extensive SCF calculations performed within this study included s, p, and d functions and predict  $2P_4$  to be 158 kJ/mol more stable than  $P_8$  as has been discussed in section III. The 3d contributions definitely tip the balance in favor of  $P_4$ . This trend is expected since the stabilizing effect of 3d functions is usually more pronounced for "strained" molecules. It is instructive to discuss this effect for the occupied  $t_2(3p)$  MO—the  $t_2$  MO arising from 3p AOs—of  $P_4$ , which plays a crucial role since one-half of the occupied MOs arising from 3p AOs ( $a_1$ ,  $t_2$ , and  $e$ , compare Figure 6 below) are of this type.

The contour diagram of a  $t_2$  MO of  $P_4$  is shown in Figure 3; its relevant features are depicted schematically in Figure 4. The  $t_2(3p)$  MOs are basically the minus combination of two-center banana bonds referring to opposite edges of the tetrahedron. Since the 3p subshells give rise to two sets of  $t_2$  orbitals, there is one variational parameter for the occupied  $t_2(3p)$  MO which may be chosen as the tilt angle  $\alpha$  defined in Figure 4. The  $t_2(3p)$  MOs are characterized by the following interactions: (i) bonding within the banana bonds which is strongest for  $\alpha = 0$ , i.e., a straight  $3p\sigma$  bond; (ii) the node passing through the molecular center (required by symmetry), which is only weakly destabilizing for  $\alpha \approx 45^\circ$  but becomes strongly destabilizing for negative  $\alpha$ ; and (iii) the nodal surface does not separate the banana bonds completely and there is a stabilizing (in phase) interaction of the outer lobes of one banana bond with the central region of the other one which is strongest for  $\alpha \approx 30^\circ$ . This is a peculiarity of tetrahedral molecules and three-membered rings (it does not occur for four-membered rings), which counteracts the destabilizing effect ii.

The contributions of 3d AOs now polarize the lobes of 3p AOs toward the molecular center, as indicated in Figure 4, thus increasing the overlap within the banana bonds and in the outer region which clearly stabilizes the  $t_2(3p)$  MO. This mechanism is especially efficient in connection with the appropriate variational adjustment of the tilt angle  $\alpha$ . No comparable effect is present for  $P_8$ .

**(d) Localized Bond Orbitals and Shared Electron Numbers (SEN).** As a summary and confirmation of the preceding dis-

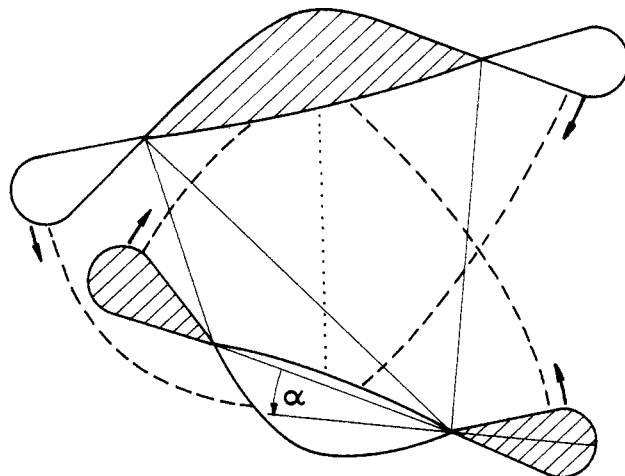


**Figure 4.** Schematic representation of bonding and antibonding effects for a  $t_2(3p)$  MO of  $P_4$  as discussed in the text. The dotted line indicates an antibonding interaction between the constituting banana bonds and the broken lines indicate a bonding interaction. The arrows indicate the polarization effected by admixture of 3d AOs. Compare also the contour diagram given in Figure 3.

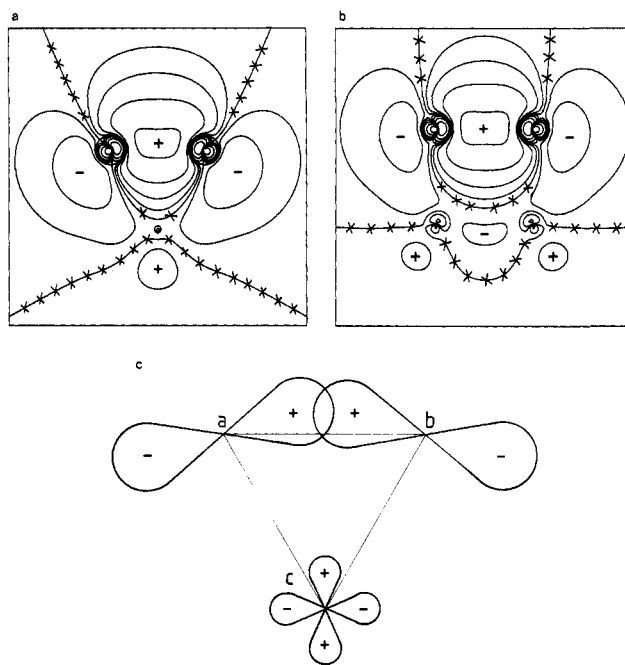


**Figure 5.** Contour lines of localized bond orbitals: (a) for  $P_4$ , in the face of the tetrahedron; (b) for  $P_8$ , in the face of the cube. The following lines are plotted: 0 (crossed),  $\pm 0.01$ ,  $\pm 0.03$ ,  $\pm 0.08$ ,  $\pm 0.2$  au. (c) Schematic representation of dominant features of a, which shows the banana bond between centers a-b and the weak  $3p\pi-3d\pi$  bond between a-c and b-c.

cussions let us finally consider the contour diagrams of localized MOs (LMO)<sup>24</sup> and the SEN provided by the population analysis based on occupation numbers.<sup>25-28</sup>

The bond orbitals shown in Figure 5 show the pronounced banana shape for  $P_4$  and a slight bending for  $P_8$  in agreement with the above discussion.

More instructive is a consideration of the nodes of LMOs which are reliable indicators of repulsions between bond (and lone pair) orbitals. The bond orbital of  $P_8$  shows in fact a nodal surface which separates it from the parallel adjacent bond, which represents bond repulsion. However, this separation is not pronounced and the

(24) Boys, S. F. *Rev. Mod. Phys.* **1960**, *32*, 296.

(25) Davidson, E. R. *J. Chem. Phys.* **1967**, *46*, 3320.

(26) Roby, K. R. *Mol. Phys.* **1974**, *27*, 81.

(27) Heinzmann, R.; Ahlrichs, R. *Theor. Chim. Acta* **1976**, *42*, 33.

(28) Ehrhardt, C.; Ahlrichs, R. *Theor. Chim. Acta* **1985**, *68*, 231.

LMO has a complicated structure at the atoms outside the bond. These features display the appreciable  $\sigma^*(3p)$  or  $\pi$  contributions to MOs of  $P_8$  discussed in subsection b.

Quite a different situation is met in  $P_4$ : the LMO, Figure 5, shows no obvious signs of repulsion effects. The dominant nodal surface connects the nodes of the 3p AOs which form the banana bond. This node and a second minor one almost meet at the external atom where the LMO is of 3d type—with small s contributions. Besides the (strong) banana bond one thus has additional weak bonding effects of  $3p\pi-3d\pi$  type between the bond atoms and the external atoms, as is shown schematically in Figure 5c. This is an unusual situation which has to be interpreted as a multicenter bonding effect. It expresses in terms of LMOs the effects discussed in subsection c: the interplay of 3d contributions and the optimal tilt angle  $\alpha$  allow a reduction of the destabilizing effect of the central node of the  $t_2(3p)$  MO and the enhancement of the bonding effects within the banana bonds and in the outer region.

The population analysis based on occupation numbers<sup>25-28</sup> characterizes the bond strength by means of the SEN referring to pairs, triples, etc., of atoms. The two-center SEN has been shown to be a reliable measure of bond strength.<sup>28</sup> The following results were obtained

$P_4$ :

$$\text{SEN(PP)} = 1.36 \quad (12)$$

$$\text{SEN(PPP)} = 0.25 \quad (13)$$

$$\text{SEN(PPPP)} = 0.15 \quad (14)$$

$P_8$ :

$$\text{SEN(PP)} = 1.15 \quad (15)$$

Multicenter SENs of  $P_8$  are small, typically 0.04. The two-center SEN, eq 12 and 15, indicate a normal bond strength for  $P_4$  and a weaker single bond in  $P_8$ . This judgment emerges from a comparison with typical SENs: strong  $\sigma$  bonds (H-H, C-H, C-C) typically have  $\text{SEN} \approx 1.4$ , weak  $\sigma$  bonds have  $\text{SEN} = 0.9$  ( $\text{Cl}_2$ ) to 0.6 ( $\text{F}_2$ ). The multicenter SENs for  $P_4$  are unusually large. Three-center SENs are typically in the order of 0.01, except for compounds such as  $\text{B}_2\text{H}_6$ , where  $\text{SEN}(\text{BHB}) = 0.7$ . The results of the population analysis are perfectly in line with the conclusions drawn in this section.

The SCF orbital energies shown in Figure 6 mainly show a markedly increased "bandwidth" of 3s and 3p bands in  $P_8$  as compared to  $P_4$ , which leads to overlapping 3s and 3p bands in  $P_8$ . This results partly from the larger number of interacting atoms in  $P_8$  and partly from increased 3s-3p interactions (hybridization) in  $P_8$  as discussed above.

## V. Summary

The so far most elaborate and most accurate calculations for  $P_2$ ,  $P_4$ , and  $P_8$  have been reported and discussed. It turns out that polarization basis sets larger than (2d1f) are required and that effects of electron correlation have to be included if reaction energies are to be computed with an accuracy of 10 kJ/mol (see

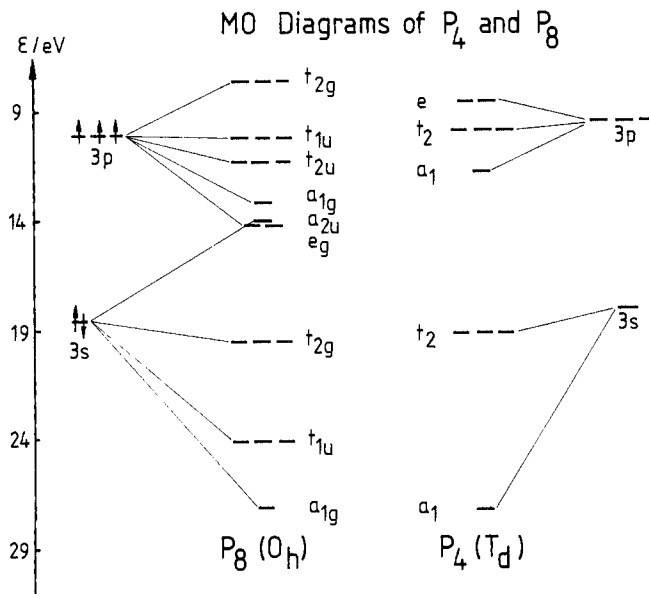


Figure 6. Computed valence shell SCF orbital energies of  $P_4$  ( $T_d$ ) and  $P_8$  ( $O_h$ ).

Tables I and II). The computed  $R_c$  for  $P_2$  and  $P_4$  on the highest level considered in this work are in excellent agreement with available experimental data.

For the stability of  $P_4$  it is essential that the strain energy caused by  $60^\circ$  angles is relatively small, only about 60 kJ/mol, since bonding mainly involves 3p AOs. The pronounced stabilization through 3d contributions which leads, in connection with the tetrahedral structure, to multicenter bonding effects is decisive. It thus appears that  $P_4$  ( $T_d$ ) is the natural molecular state of phosphorous, as is  $\text{As}_4$  for arsenic. This reasoning does not only hold for tetrahedral  $P_4$ , it basically carries over to rationalize the stability of  $P_3$  rings in general.

Cubic  $P_8$  is found to be higher in energy than  $2P_4$ , which is partly attributed to the repulsion of parallel PP bonds.<sup>2</sup> This is consistent with the large PP distance computed for cubic  $P_8$ ,  $R_c = 4.33a_0 = 229$  pm, which is already on the way to the value found in the metallic primitive cubic modification of phosphorus,  $R_c = 238$  pm. It is interesting to note that black phosphorus, the most stable solid state form reduces bond repulsions by means of bond angles of  $96.5^\circ$  and  $102^\circ$ , which keep the bonds in the double layer apart (in a localized description).

**Acknowledgment.** The authors thank Prof. V. Staemmler for a valuable discussion and H. Schiffer for helpful assistance in performing the calculations. The computations were performed at the "Rechenzentrum der Universität Karlsruhe"; the present work has greatly benefitted from the excellent service provided by this institution. This work has been supported in part by the Fonds der Chemischen Industrie.

Registry No.  $P_2$ , 12185-09-0;  $P_4$ , 12185-10-3;  $P_8$ , 78998-14-8.